PHYSICAL REVIEW B **80**, 081409(R) (2009)

Decay mechanisms of excited electrons in quantum-well states of ultrathin Pb islands grown on Si(111): Scanning tunneling spectroscopy and theory

I-Po Hong,[1] Christophe Brun,[1] François Patthey,[1] I. Yu. Sklyadneva,[2,3] X. Zubizarreta,[2,4] R. Heid,[5] V. M. Silkin,[2,4] P. M. Echenique,[2,4] K. P. Bohnen,[5] E. V. Chulkov,[2,4] and Wolf-Dieter Schneider[1]

[1]*École Polytechnique Fédérale de Lausanne (EPFL), Institut de Physique de la Matière Condensée, CH-1015 Lausanne, Switzerland*

[2]*Donostia International Physics Center (DIPC), Paseo de Manuel Lardizabal, 4, San Sebastián/Donostia, 20018 Basque Country, Spain*

[3]*Institute of Strength Physics and Materials Science, Prospekt Academicheski 2/1, 634021 Tomsk, Russia*

[4]*Departamento de Física de Materiales and Centro Mixto CSIC-UPV/EHU, Facultad de Ciencias Químicas, UPV/EHU, Apartado 1072, San Sebastián/Donostia, 20080 Basque Country, Spain*

[5]*Forschungszentrum Karlsruhe, Institut für Festkörperphysik, P.O. Box 3640, D-76021 Karlsruhe, Germany*

(Received 5 August 2009; published 20 August 2009)

Using low-temperature scanning tunneling spectroscopy at 5 and 50 K, we studied the linewidth of unoccupied quantum-well states in ultrathin Pb islands, grown on Si(111) on two different Pb/Si interfaces. A quantitative analysis of the differential conductance spectra allowed us to determine the electron-electron (*e*-*e*), electron-phonon (*e*-ph) and the interface and defect contributions to the lifetime. Layer-dependent *ab initio* calculations of the *e*-ph linewidth contribution are in excellent agreement with the data. Importantly, the sum of the calculated *e*-*e* and *e*-ph lifetime broadening follows the experimentally observed quadratic energy dependence.

DOI: 10.1103/PhysRevB.80.081409 PACS number(s): 73.21.Fg, 68.37.Ef, 73.50.Gr, 79.60.Dp

Understanding the basic processes governing the decay of elementary electronic excitations in metals and at metal surfaces is important because these excitations play a major role in a large variety of chemical and physical phenomena, including chemical reactions or catalysis at surfaces, molecule-surface interactions and transport properties. A clear picture of the decay mechanisms occurring in several types of bulk metals (simple, noble, paramagnetic and some ferromagnetic transition metals) has been obtained.[1] The analysis of the dynamics of surface and image potential states (SS and IPS) also clarified the decay processes at the surface of various metals.[1]

Thin metal films are interesting from a fundamental point of view and for technological applications. In a thin metal film electrons occupy discrete eigenstates with a quantized wave vector perpendicular to the surface, known as quantum-well states (QWS).[2–4] These states, forming two-dimensional (2D) bands, are intermediate between bulk states and SS. Due to technical limitations, few studies have reported so far detailed contributions to the QWS lifetime. For example, photoemission (PES), two-photon PES (2PPE) and time-resolved 2PPE (TR-2PPE) require homogeneous films over macroscopic areas. Nevertheless, the electron-electron (*e*-*e*) contribution $\Gamma_{e\text{-}e}$ was determined in Ag/Fe(100) by PES and TR-2PPE (Refs. 5 and 6) and in Pb/Si(111).[7] The electron-phonon (*e*-ph) contribution $\Gamma_{e\text{-ph}}$ was extracted by PES in Ag/Fe(100) (Ref. 5) and in Ag/Cu(111).[8] Layer-dependent or electronic structure dependent *e*-ph contributions were also reported.[9–12]

Scanning tunneling spectroscopy (STS) benefits from being a local probe but suffers from the lack of **k** resolution. However, detailed quantitative lifetime studies were achieved for SS (Refs. 13–16) and IPS.[17] Up to now only one STS study reported a quantitative linewidth analysis of a QWS metal system, Yb(111)/W(110).[18] A quadratic energy dependence of the linewidth was found, in agreement with three-dimensional (3D) Fermi-liquid (FL) theory, and a large *e*-ph coupling constant. Both results were subsequently questioned by a TR-2PPE study on bulk Yb.[19] These controversial results illustrate the difficulties and limits encountered in STS experiments to retrieve reliable quantitative QWS lifetime data.

In this Rapid Communication we present a detailed low-temperature STS study of the linewidth of unoccupied QWS in Pb islands of thicknesses 7–22 monolayers (MLs) grown on Si(111). Using a simple model with tunneling allowed through a trapezoidal barrier for a set of discrete QWS, a quantitative analysis of the differential conductance dI/dV spectra allows us to determine the QWS lifetime broadening as a function of energy, and the *e*-ph contribution between 5 and 50 K. The interface and defect scattering contribution to the QWS linewidth from the disordered Pb/Si(111)-7×7 (hereafter 7×7) interface is 90 meV larger than the one from the crystalline Pb-$\sqrt{3}\times\sqrt{3}$/Si(111) (in short Pb$\sqrt{3}$) interface. Layer-dependent *ab initio* calculations of $\Gamma_{e\text{-ph}}$ were performed for 4–10 ML free-standing Pb(111) films, taking full account of the quantum-size effects on the electron and phonon band structures and on the *e*-ph coupling.[20,21] The theoretical results are in very good agreement with the experimental findings. $\Gamma_{e\text{-}e}$ was estimated from *ab initio* calculation of $\Gamma_{e\text{-}e}$ for the parent bulk band dispersing along Γ-L.[20] The calculated $\Gamma_{e\text{-ph}}+\Gamma_{e\text{-}e}$ is convincingly fitted by a quadratic equation in agreement with the experimental results. The effect of spin-orbit coupling (SOC) on the electronic band energies and on $\Gamma_{e\text{-}e}$ is small in the probed energy range. The *e*-ph coupling constant calculated for the unoccupied QWS, $\lambda\simeq1.45-1.60$, is generally larger than λ calculated at the Fermi energy (E_F) for the corresponding films.[21]

The measurements were performed in a homebuilt scanning tunneling microscope (STM) operated at 50 and 5 K in ultrahigh vacuum using cut PtIr tips.[22] dI/dV spectra were measured using currents of $200\leq I\leq500$ pA, with open

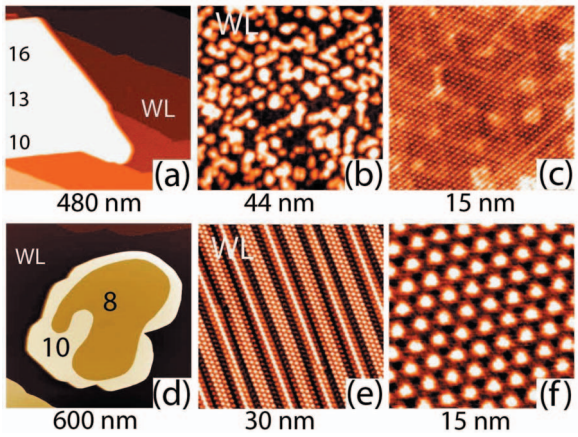

FIG. 1. (Color) STM images showing typical features of Pb islands grown on Si(111)-7×7 (a)–(c) and on Pb-$\sqrt{3}\times\sqrt{3}$/Si(111) (d)–(f). (a) and (d) Large scale overview. The indicated island thickness includes the wetting layer (WL). (b) Disordered WL $\simeq$1 ML high. (c) Atomic resolution of the surface Pb lattice. Buried 7×7 interface seen through a 8ML island. (e) High resolution of the crystalline Pb WL, a saturated Pb ML. (f) Moiré pattern on a 8 ML island.

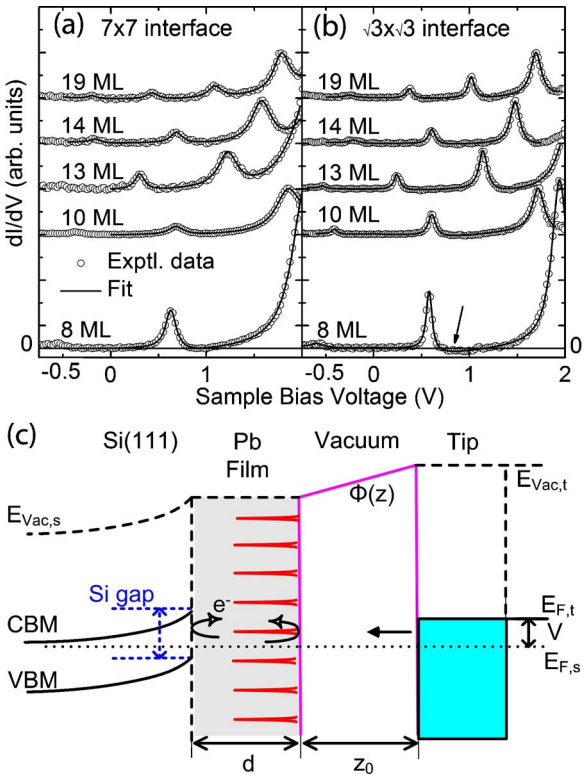

FIG. 2. (Color online) Experimental (dots) and calculated (full line) dI/dV spectra measured at 5 K by tunneling to a large atomically flat Pb island of selected thickness grown on (a) Si(111)-7×7 and (b) Pb-$\sqrt{3}\times\sqrt{3}$/Si(111). The arrow indicates negative differential conductance. (c) Schematic energy diagram of the tunnel junction used to model the experiment. CBM: conductance band minimum, VBM: valence-band maximum, d: film thickness, z_0: vacuum gap. $E_{F,s}(E_{F,t})$: sample (tip) Fermi level. $E_{vac,s}(E_{vac,t})$: sample (tip) vacuum level. $\Phi(z)$: vacuum potential drop between tip and sample. V: tip-sample bias voltage.

feedback loop via lock-in technique with a modulation amplitude of 10 mV_{pp} at a frequency of 1.4 kHz. Pb was thermally evaporated on the Si(111)-7×7 or on the Pb$\sqrt{3}$ substrate kept at room temperature favoring the growth of Pb single crystals with their (111) axis perpendicular to the surface.[23,24] All dI/dV measurements were performed on large Pb islands far from steps or island boundaries to avoid additional broadening of the QWS linewidths.

Figure 1 shows Pb islands grown on 7×7 (a)–(c) and Pb$\sqrt{3}$ (d)–(f). Thicknesses given in ML include the WL. Large islands of several hundreds of nm are formed. Figure 1(c) reveals the buried Si-7×7 interface superimposed with the atomic resolution of the Pb lattice indicating that the island surface is atomically flat.[25,26] As shown in Fig. 1(b) the Pb WL formed on Si-7×7 is disordered. In contrast, a crystalline topography is observed both on the island and on the WL on Pb$\sqrt{3}$ [see Figs. 1(d)–1(f)]. The WL displays a striped-incommensurate superstructure [see Fig. 1(e)] corresponding to a saturated Pb phase.[27,28] Figure 1(f) shows a Moiré pattern on a 8 ML island, caused by interfacial strain due to the difference between the Si and Pb lattice constant.[29]

Figure 2 presents single dI/dV spectra obtained at 5 K on Pb islands of selected thickness. Remarkably, the spectra consist of prominent maxima located at the QWS energies. Previous STS studies of QWS in Pb/Si(111),[25] in Yb/W(110),[18] and of lanthanide SS (Ref. 30) suggested that this line shape results from a high effective mass near the 2D subbands onset, which was confirmed by PES for Pb/Si(111).[31] The measured QWS energies are similar for both interfaces, with larger dispersion on the disordered one.[32] If the WL thickness is assumed to be 1 ML, agreement occurs between calculated QWS energies for free-standing films[33] and our experimental data for thicknesses $\geq$17 ML.[32] At smaller thickness a systematic deviation exists, increasing with decreasing thickness. A comparison between the spectra shown in Figs. 2(a) and 2(b) reveals a considerable narrowing of the QWS linewidths on the Pb$\sqrt{3}$ interface with respect to the ones on 7×7.

To extract the intrinsic QWS linewidth, dI/dV is modeled based on a 1D WKB approach with a trapezoidal potential barrier.[25,34] Figure 2(c) depicts the schematic energy diagram of the junction. The Pb island density of states (DOS) ρ_s is simulated as a series of Lorentzian peaks, whereas the tip DOS ρ_t is assumed to be constant. As a function of bias voltage V, I is written[35]

$$I_{WKB}(V) = \int_{-\infty}^{\infty} \left[\rho_s(\epsilon)\rho_t(\epsilon - eV)[f(\epsilon) - f(\epsilon - eV)] \exp\left(-\frac{2}{\hbar} \int_0^{z_0} \mathrm{Re}\left\{ \sqrt{2m\left[\Phi - \epsilon + \left(1 - \frac{z}{z_0}\right) eV \right]} \right\} dz \right) \right] d\epsilon. \quad (1)$$

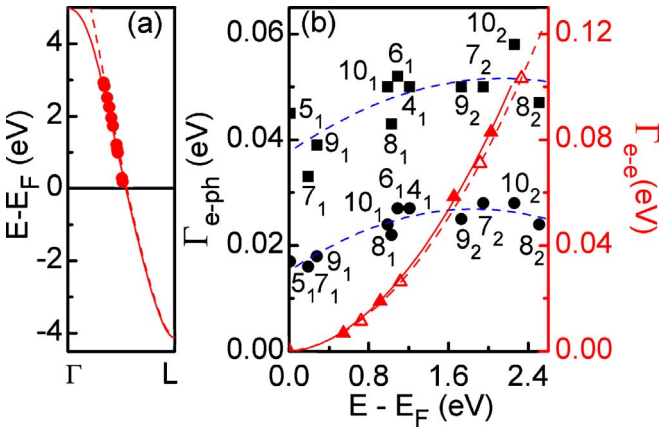

FIG. 3. (Color online) (a) Calculated dispersion of the electronic band crossing E_F along Γ-L for bulk Pb without spin-orbit coupling (with SOC): dashed (solid) line. Dots: computed QWS energies. (b) Calculated $\Gamma_{e\text{-}e}$ and $\Gamma_{e\text{-ph}}$ for unoccupied QWS as a function of energy. $\Gamma_{e\text{-}e}$ without SOC (with SOC): open (full) triangles. $\Gamma_{e\text{-ph}}$ at 5 K (50 K): dots (squares) with their fit. In $n_m(n=4,\ldots,10;\ m=1,2)n$ is the film number of monolayers, and m is the QWS number counted from E_F.

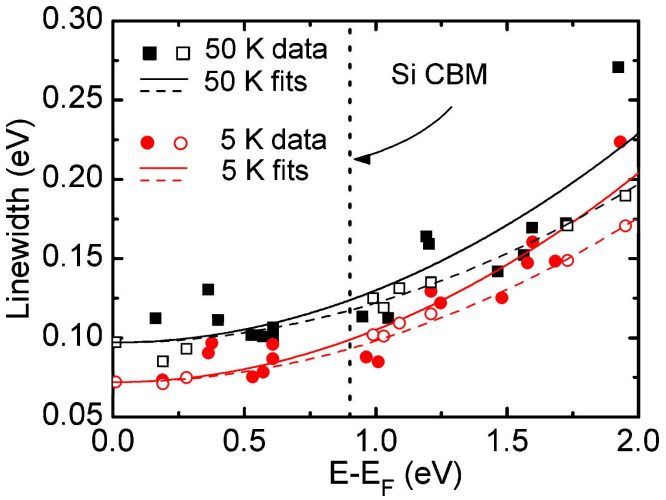

FIG. 4. (Color online) Linewidth versus energy of unoccupied QWS in Pb islands grown on Pb-$\sqrt{3}\times\sqrt{3}$/Si(111) measured at 5 (50) K: full dots (full squares). The data are fitted according to 3D Fermi-liquid theory (continuous lines). Theoretical linewidth $\Gamma_{e\text{-}e}+\Gamma_{e\text{-ph}}$ at 5 (50) K: open dots (open squares) with corresponding fits (dashed lines). For easier comparison the theoretical data have been shifted up so that the theoretical fits coincide with the experimental ones at low energy. The linewidth difference $\Delta\Gamma_{e\text{-ph}}\simeq 25$ meV between the 50 and 5 K fit to the experimental data agrees very well with the corresponding calculated difference, yielding the QWS e-ph coupling constant $\lambda\simeq 1.45-1.60$. Silicon conduction band minimum is indicated.

The nonzero conductance observed between the QWS is modeled by an additional exponential term. This analysis describes convincingly the STS data [see Figs. 2(a) and 2(b)].

Possible causes of extrinsic broadening are the transmission to the substrate, the QWS lateral dispersion and the ac voltage modulation. The latter contributes a few mV. Following Ref. 5, the reflectivity of both Pb/Si interfaces was found to be very close to one in the studied voltage range, contributing to negligible broadening. As symmetric QWS peaks are observed on both interfaces, tunneling of electrons with finite $k_\parallel$ should contribute less than 10 meV to the linewidth.[18,30]

Consequently, extrinsic linewidth contributions were neglected in the following analysis. $\Gamma(T,E)$ was further decomposed as follows:

$$\Gamma(T,E)=\Gamma_0+\Gamma_{e\text{-}e}(E)+\Gamma_{e\text{-ph}}(E,T), \qquad (2)$$

where T is the temperature and E is the QWS energy. $\Gamma_{e\text{-}e}(E)$ is the e-e interaction term and $\Gamma_{e\text{-ph}}(E,T)$ reflects the e-ph scattering. Γ_0, independent of T and E, describes interface and defects scattering.

Figure 3(a) shows that our calculated QWS energies are almost lying on the parent bulk band. The calculated effective masses are very close to the free electron mass. Figure 3(b) shows $\Gamma_{e\text{-}e}(E)$ computed for bulk band energy equal to the QWS energy with and without SOC. A quadratic dependence $\Gamma_{e\text{-}e}=\alpha(E-E_F)^2$ is found, leading to $\alpha=0.023$ eV^{-1} with SOC (0.021 without), which are very close to $\alpha=0.02$ eV^{-1} obtained when treating bulk Pb as a free electron gas ($r_s=2.30$ a.u). Hence, in the probed energy range, the SOC effect on band (QWS) energies and on $\Gamma_{e\text{-}e}$ is small. Figure 3(b) shows $\Gamma_{e\text{-ph}}$ versus QWS energy calculated for 5 and 50 K. It varies with QWS energy, but the difference between the averaged $\Gamma_{e\text{-ph}}$'s (dashed lines), $\Delta\Gamma_{e\text{-ph}}=\Gamma_{e\text{-ph}}(50K)-\Gamma_{e\text{-ph}}(5K)$, remains nearly constant, increasing from 23 meV close to E_F to 26 meV at higher energies. Since the energy dependence of $\Gamma_{e\text{-}e}$ is much stronger than that of $\Gamma_{e\text{-ph}}$, their sum $\Gamma_{e\text{-}e}+\Gamma_{e\text{-ph}}$, is fitted reasonably well by a quadratic equation with $\alpha=0.025$ eV^{-1} (0.026) at 50 (5) K (see Fig. 4).

Figure 4 shows Γ versus energy measured at 50 and 5 K on Pb$\sqrt{3}$ with the theoretical $\Gamma_{e\text{-}e}+\Gamma_{e\text{-ph}}$. Both experimental data sets are well fitted by 3D FL theory: $\Gamma(E)=\alpha(E-E_F)^2$, yielding the same value $\alpha=0.033$ eV^{-1}. The difference $\Delta\Gamma_{e\text{-ph}}\simeq 25$ meV between the 50 and 5 K fit to the experimental data yields an estimate of the average e-ph contribution to the QWS lifetime in excellent agreement with the theoretical $\Delta\Gamma_{e\text{-ph}}\simeq 23-26$ meV. A similar analysis was conducted on the 7×7 interface, which showed a larger linewidth dispersion due to disorder at this interface. In contrast to the crystalline Pb$\sqrt{3}$, the linewidths increase with decreasing thickness ($\simeq$20 meV from 22 to 7 ML). This linewidth variation was taken into account before $\Gamma_{e\text{-}e}$, $\Gamma_{e\text{-ph}}$, and Γ_0 were extracted. Γ_0 is found to be about 90 meV larger on 7×7 (see Fig. 2). $\alpha=0.028$ eV^{-1} at 50 K (0.037 at 5 K), $\Delta\Gamma_{e\text{-ph}}\simeq 26$ meV, which is consistent with the values obtained on Pb$\sqrt{3}$ and with the theoretical results.

The large $\Delta\Gamma_{e\text{-ph}}$ measured on both interfaces reflect a strong e-ph coupling of the QWS in Pb thin films. A Debye model[36] with $\lambda_{bulk}=1.55$ yields $\Delta\Gamma_{e\text{-ph}}=23$ meV, which is close to the measured averaged $\Delta\Gamma_{e\text{-ph}}$. The present *ab initio* calculations yield for most QWS $1.45\leq\lambda\leq 1.6$. These values are larger than those computed for Pb thin films at E_F (Ref. 21) but close to λ_{bulk} at E_F.[36] The excellent agreement between theoretical and experimental e-ph coupling terms

allows us to discriminate among the three contributions of Eq. (2). For 7–22 ML films the resulting electronic mean free path at E_F, $v_F\tau_0(\Gamma_0=\hbar/\tau_0)$ can be estimated for both interfaces, yielding 3–4 nm for 7×7 and 11 nm for Pb$\sqrt{3}$ [Fermi velocities v_F are determined from the reconstructed band dispersion along Γ-L (Ref. 32)].

In a previous Yb/W(110) QWS linewidth study by STS, the neglect of the interface and defect scattering term in the low-energy residual linewidth and a lack of temperature-dependent measurements, led to a strong e-ph coupling constant $\lambda\simeq1.6-2.8$.[18] In contrast, TR-2PPE measurements of the parent d band in bulk Yb found $\lambda\simeq0.4$.[19] Moreover TR-2PPE results together with *ab initio* calculations reported a linewidth energy dependence far from being quadratic.[19]

In conclusion, the combination of high-accuracy temperature-dependent STS experiments with *ab initio* calculations allowed us to identify individual QWS in single ultrathin metal islands, to separate consistently the different decay mechanisms of these electronic excitations and to determine the QWS electron-phonon coupling strength. These achievements open up an avenue toward detailed investigations of the decay processes of electronic excitations on a local scale, e.g., of individual supported molecules, clusters or other nanostructures.

We thank J. H. Dil, P. S. Kirchman, U. Bovensiepen, and T.-C. Chiang for stimulating discussions. Financial support from the Swiss National Science Foundation, the University of the Basque Country, the Departamento de Educación del Gobierno Vasco, and the Spanish Ministerio de Ciencia y Tecnología (MCyT) (Grant No. FIS 2004-06490-C03-01) is acknowledged.

[1] E. V. Chulkov, A. G. Borisov, J. P. Gauyacq, D. Sánchez-Portal, V. M. Silkin, V. P. Zhukov, and P. M. Echenique, Chem. Rev. **106**, 4160 (2006).
[2] R. C. Jaklevic, John Lambe, M. Mikkor, and W. C. Vassell, Phys. Rev. Lett. **26**, 88 (1971).
[3] T.-C. Chiang, Surf. Sci. Rep. **39**, 181 (2000).
[4] M. Milun, P. Pervan, and D. P. Woodruff, Rep. Prog. Phys. **65**, 99 (2002).
[5] J. J. Paggel, T. Miller, and T.-C. Chiang, Science **283**, 1709 (1999).
[6] S. Ogawa, H. Nagano, and H. Petek, Phys. Rev. Lett. **88**, 116801 (2002).
[7] P. S. Kirchmann and U. Bovensiepen, Phys. Rev. B **78**, 035437 (2008).
[8] K. Takahashi, A. Tanaka, M. Hatano, H. Sasaki, S. Suzuki, and S. Sato, Surf. Sci. **433-435**, 873 (1999).
[9] M. Kralj, A. Siber, P. Pervan, M. Milun, T. Valla, P. D. Johnson, and D. P. Woodruff, Phys. Rev. B **64**, 085411 (2001).
[10] J. J. Paggel, D.-A. Luh, T. Miller, and T.-C. Chiang, Phys. Rev. Lett. **92**, 186803 (2004).
[11] Y. F. Zhang, J. F. Jia, T. Z. Han, Z. Tang, Q. T. Shen, Y. Guo, Z. Q. Qiu, and Q. K. Xue, Phys. Rev. Lett. **95**, 096802 (2005).
[12] S. Mathias, M. Wiesenmayer, M. Aeschlimann, and M. Bauer, Phys. Rev. Lett. **97**, 236809 (2006).
[13] J. Li, W. D. Schneider, R. Berndt, O. R. Bryant, and S. Crampin, Phys. Rev. Lett. **81**, 4464 (1998).
[14] L. Bürgi, O. Jeandupeux, H. Brune, and K. Kern, Phys. Rev. Lett. **82**, 4516 (1999).
[15] J. Kliewer, R. Berndt, E. V. Chulkov, V. M. Silkin, P. M. Echenique, and S. Crampin, Science **288**, 1399 (2000).
[16] L. Vitali, P. Wahl, M. A. Schneider, K. Kern, V. M. Silkin, E. V. Chulkov, and P. M. Echenique, Surf. Sci. Lett. **523**, L47 (2003).
[17] P. Wahl, M. A. Schneider, L. Diekhöner, R. Vogelgesang, and K. Kern, Phys. Rev. Lett. **91**, 106802 (2003).
[18] D. Wegner, A. Bauer, and G. Kaindl, Phys. Rev. Lett. **94**, 126804 (2005).
[19] V. P. Zhukov, E. V. Chulkov, P. M. Echenique, A. Marienfeld, M. Bauer, and M. Aeschlimann, Phys. Rev. B **76**, 193107 (2007).
[20] See EPAPS Document No. E-PRBMDO-80-R26932 for details of this kind of calculation, which can be found in Ref. 1. For more information on EPAPS, see http://www.aip.org/pubservs/epaps.html.
[21] C. Brun, I. Po Hong, F. Patthey, I. Y. Sklyadneva, R. Heid, P. M. Echenique, K. P. Bohnen, E. V. Chulkov, and W. D. Schneider, Phys. Rev. Lett. **102**, 207002 (2009).
[22] R. Gaisch, J. K. Gimzewski, B. Reihl, R. R. Schlittler, M. Tschudy, and W. D. Schneider, Ultramicroscopy **42-44**, 1621 (1992).
[23] M. Jalochowski and E. Bauer, Phys. Rev. B **38**, 5272 (1988).
[24] H. H. Weitering, D. R. Heslinga, and T. Hibma, Phys. Rev. B **45**, 5991 (1992).
[25] I. B. Altfeder, K. A. Matveev, and D. M. Chen, Phys. Rev. Lett. **78**, 2815 (1997).
[26] I. B. Altfeder, D. M. Chen, and K. A. Matveev, Phys. Rev. Lett. **80**, 4895 (1998).
[27] L. Seehofer, G. Falkenberg, D. Daboul, and R. L. Johnson, Phys. Rev. B **51**, 13503 (1995).
[28] M. Hupalo, J. Schmalian, and M. C. Tringides, Phys. Rev. Lett. **90**, 216106 (2003).
[29] I. B. Altfeder, V. Narayanamurti, and D. M. Chen, Phys. Rev. Lett. **88**, 206801 (2002).
[30] A. Bauer, A. Mühlig, D. Wegner, and G. Kaindl, Phys. Rev. B **65**, 075421 (2002).
[31] J. H. Dil, J. W. Kim, T. Kampen, K. Horn, and A. R. H. F. Ettema, Phys. Rev. B **73**, 161308(R) (2006).
[32] I.-P. Hong *et al.* (to be published).
[33] C. M. Wei and M. Y. Chou, Phys. Rev. B **66**, 233408 (2002).
[34] E. L. Wolf, *Principles of Electron Tunneling Spectroscopy* (Oxford University Press, New York, 1985).
[35] We assume that $z_0=10$ Å with sample and tip work functions equal to 4 eV (Ref. 37 and 38).
[36] G. Grimvall, *The Electron-Phonon Interaction in Metals* (North-Holland, New-York, 1981).
[37] P. S. Kirchmann, M. Wolf, J. H. Dil, K. Horn, and U. Bovensiepen, Phys. Rev. B **76**, 075406 (2007).
[38] H.-C. Ploigt, C. Brun, M. Pivetta, F. Patthey, and W. D. Schneider, Phys. Rev. B **76**, 195404 (2007).